

Thermal Flow Measurements at $Gr/Re^2 \gg 1$ by Silicon Anemometry

Michael J. A. M. van Putten, Maurice H. P. M. van Putten, and Anton F. P. van Putten

Abstract—We present the first characteristics of air flow measurements in the mixed convective region with strong buoyancy effects ($Gr/Re^2 \gg 1$), using a thermal silicon double-Wheatstone-bridge vector sensor. The Alternating Direction Method is applied to eliminate additive drift influences. The upper limit on the mixed convective region is experimentally defined to be given by $Gr/Re^2 = [0.3-0.8]$. Flow velocity measurements of down to 1 mm/s (Reynolds ≈ 0.3) are realized with an accuracy better than 98%.

Index Terms— Alternating Direction Method (ADM), mixed convection, silicon flow sensor, thermal flow measurements.

I. INTRODUCTION

Thermal flow sensors measure the flow of a medium by detecting changes in the forced convective heat transport from the sensor. In general, three processes play a role in the heat transport from the sensor to the fluid:

- 1) radiation;
- 2) free convection;
- 3) forced convection.

While at high velocities the contributions of 1) and 2) can be neglected, the lower limit for conventional thermal flow measurements is due to the relative increase of the contribution of 2) at lower (forced) flow velocities. This region is known as the *mixed convective region* and is characterized by a significant mutual interaction between the temperature field and the velocity field: the temperature distribution depends on the velocity distribution and the velocity distribution depends on the temperature distribution. In this flow region, therefore, there exists a relevant interaction between the buoyancy forces, caused by the temperature induced density differences and the inertial forces induced by the forced convective flow.

Typically, therefore, thermal flow sensors show a marked decrease in sensitivity at low velocities due to the natural or free convective flow generated by the flow sensor. At these low velocities, this free convective flow tends to mask any low-velocity forced convection cooling, resulting in a flattening of the lower end of the calibration curves. For instance, the lowest limit for accurate air flow measurements with conventional hot wires is at about 0.15–0.20 m/s [1], [2] and the lower limits

for silicon sensor anemometers is reported to be approximately 0.3–1 m/s [3]–[6].

The temperature and velocity distributions in this mixed convective region are characterized by three dimensionless numbers, Reynolds number Re , Prandtl number Pr , and Grashof number Gr , given by

$$Re = \frac{v_0 L}{\nu} \quad (1)$$

with

- v_0 mean flow velocity;
- ν kinematic viscosity;
- L characteristic length;

$$Gr = \frac{gL^3\beta\Delta T}{\nu^2} \quad (2)$$

with

- g gravity force;
- β coefficient of thermal expansion;
- ΔT fluid-sensor temperature difference;

and

$$Pr = \frac{C_p \mu}{\lambda} \quad (3)$$

where

- C_p specific heat at constant pressure;
- μ dynamic viscosity;
- λ thermal conductivity.

For gases, $Pr \approx 0.7 = \text{constant}$.

Similar to the classical, two-dimensional (2-D) analytical analysis of Sparrow *et al.* [7], the ratio of the buoyancy forces and the inertial forces is expressed as

$$\frac{gL^3\beta\Delta T/\nu^2}{v_0^2 L^2/\nu^2} = \frac{Gr}{Re^2} \quad (4)$$

where L is the characteristic length of the hot plate.

In their analysis, Re_l and Gr_l are defined in terms of the length of the plate, l . Throughout our paper, the Grashof and Reynolds number apply to this characteristic length; for notational simplicity, the subscript will be dropped.

In this paper, we study a thermal silicon integrated double Wheatstone bridge vector sensor with characteristic length $L = 4 \times 10^{-3}$ m in its application to ultralow airflow measurements at room temperature, with mean velocities ranging from 1 to 25 mm/s ($0.3 < Re < 7$). It will be shown that in this region there is a significant contribution of the buoyancy forces to the flow field.

Manuscript received June 1, 1998; revised February 22, 1999.

M. J. A. M. van Putten is with the Faculty of Applied Physics, Kramers Laboratorium voor Fysische Technologie, Delft University of Technology, 2628 BW Delft, The Netherlands (e-mail: michel@klft.tn.tudelft.nl).

M. H. P. M. van Putten is with the Department of Mathematics, Massachusetts Institute of Technology, Cambridge, MA 02139 USA.

A. F. P. van Putten is with ANMAR Research Labs, 5632 BD, Eindhoven, The Netherlands.

Publisher Item Identifier S 0018-9456(99)04990-6.

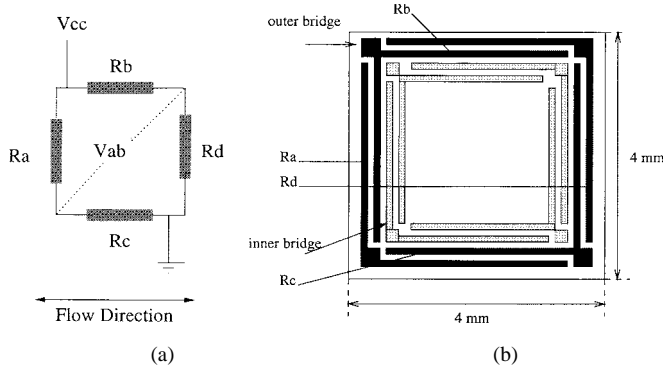


Fig. 1. (a) Schematic drawing of the sensor configuration. (b) Illustration of the two Wheatstone bridges integrated on silicon. Dimensions are 4×4 mm. The inner bridge is the heater bridge, while the outer bridge is the measurement bridge.

The first part of our experimental study will define the mixed flow region for our sensor. The second part discusses ultralow flow measurements in the mixed convective region with dominating buoyancy effects.

II. THEORY AND METHODS

A. Principle of Operation of the Flow Sensor

Thermal flow sensors measure the flow of a medium by detecting changes in the convective heat transport from the sensor to the moving fluid. In our sensor design the flow signal is contained in the gradient of a 2-D temperature distribution, $T(x, y)$ on the chip surface which is a function of the convective heat transfer to the flowing medium.

The sensor consists of a silicon integrated double Wheatstone bridge, as shown in Fig. 1. The outer bridge is the actual measurement bridge, driven by a constant current source; the inner bridge is the heater bridge.

The reference voltage at the measurement bridge, V_{cc} is kept constant and equal to a reference voltage, V_{ref} , by application of thermal feedback, as illustrated in Fig. 2. This is realized by driving the heater bridge by the output of the OpAmp II, where the feedback loop is created by thermal conduction in the substrate. The current I_1 is the current through R_a and R_c ; the current labeled I_2 is the current through the resistors R_b and R_d . The output of the first OpAmp I, contains the flow signal, V_{out} . This principle of “thermal feedback” assures both a constant reference voltage and a constant current in the outer bridge, thereby realizing a constant-current-constant-voltage biasing [8]–[11] and therefore a constant dissipation in the measurement bridge.

During flow conditions, the value of the resistances in the measurement bridge will change due to the induced temperature gradient on the chip surface in the presence of a finite heat transfer coefficient. Setting the change in the two resistors perpendicular to the flow to ΔR_a and ΔR_d , respectively, it can be shown [11] that it holds for the output signal of the sensor, $V_{out}(\eta)$, that

$$V_{out}(\eta) = \frac{V_{cc}}{4} \eta \quad (5)$$

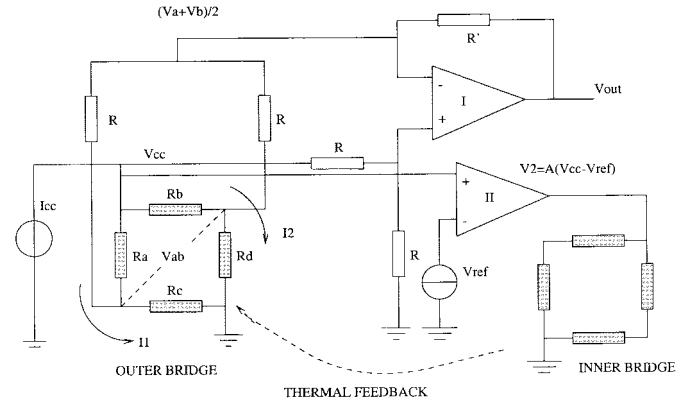


Fig. 2. Principle of thermal feedback and applied electronics.

where η is given by

$$\eta = \frac{\Delta R_a - \Delta R_d}{2R} \quad (6)$$

and V_{cc} is the voltage over the measurement bridge (cf. Fig. 1). Since for flows in the $+x$ direction, $\Delta R_a > \Delta R_d$, and vice versa, a *vector* sensor is realized. A discussion of the precise relationship between the flow and the changes in the value of the resistors R_a and R_d is beyond the scope of this paper. Summarizing, two phenomena occur when a forced convective flow is present: first, there is an increase in the amount of transferred heat, which is compensated by an increase in heat production by the heater bridge to ensure constant dissipation in the measurement bridge (global variations or zero-th order effects). Secondly, a small temperature gradient is set up across the chip surface that contains information about both the direction and strength of the flow field (nonuniform variations or first order effects).

B. The Alternating Direction Method

In the measurement of a physical process, we can in general state that

$$V = \gamma \Theta + E(U_1, U_2, \dots, U_n) \quad (7)$$

where Θ is the measurand, γ accounts for multiplicative drift influences and the function E accounts for the additive drift, where U_i can be any form of physical energy that influences V , but is different from the measurand. In the case of flow measurements, U_i can include temperature, aging, electromagnetic radiation, natural convection, radiation, etc.

The applied flow sensor is a vector sensor, which implies that the sign of the output signal is a function of the orientation of the measurand Θ with respect to the sensor, as discussed in the former section. For additive drift influences, however, the sensor shows *isotropic* behavior. This forms the basic prerequisite for application of the Alternating Direction Method (ADM). This anisotropic characteristic of the sensor makes it possible to measure two different sensor signals, V_t^A at time t and $V_{t+\Delta t}^B$ at time $t = t + \Delta t$, depending on the two relative orientations A and B of the sensor with respect to the measurand. Therefore, in measurement A we have

$$V_t^A = \gamma \Theta_t^A + E_t(U_1, U_2, \dots, U_n) \quad (8)$$

and in measurement B we have

$$V_{t+\Delta t}^B = \gamma \Theta_{t+\Delta t}^B + E_{t+\Delta t}(U_1, U_2, \dots, U_n). \quad (9)$$

Due to the anisotropic characteristics of the sensor, and assuming, that Θ is constant in the interval Δt , it holds that

$$\Theta_t^A = -\Theta_{t+\Delta t}^B. \quad (10)$$

Notice that these two partial measurements introduce two different states of the sensor in the input energy domain Θ , but similar states in the energy domains U_i . Subtraction of (9) from (8) yields

$$V_{ADM} = 2\gamma\Theta + \epsilon \quad (11)$$

where the additive drift, ϵ , has been reduced to

$$\epsilon = \frac{\partial E}{\partial t} \Delta t \quad (12)$$

with Δt the measurement interval between measurement A and B .

ADM can be realized by either turning the sensor 180° or by changing the direction of the flow. For an extensive discussion of ADM, we refer the reader to [12]–[14].

C. Experimental Setup I

Since the flow and temperature field adjacent to the hot plate define the temperature gradient on the chip surface, which in turn defines the sensor output signal, the sensor signal directly represents a net combined effect of the forced and free convection.

Buoyancy forces arise in a gravity field due to differences in density, the latter being caused by changes in the temperature, and will therefore always be directed opposite to the gravity vector. By realizing different orientations of the forced flow component with respect to the gravity vector, different relative orientations of the free convective forces and the forced convective forces are realized.

In our study, five different orientations were studied, as is illustrated in Fig. 3. Flow velocities with a component in the axial direction of the tube will be detected by the sensor. First, measurements were carried out for three horizontal orientations, where the forced convective flow is at right angles with the free convective forces generated by the hot plate. This was studied both with two vertical orientations of the hot plate and a horizontal orientation of the hot plate. We will further designate as *aiding flows* those flows for which the buoyancy force has a positive component in the direction of the free stream velocity. This is realized by a vertical orientation of the duct, where the forced flow is opposite to the gravity vector. Those flows for which the buoyancy force has a component opposite to the free stream velocity will be designated as *opposing flows*, which is realized by a vertical orientation of the duct, but now with the forced flow imposed in the same direction as the gravity vector.

The sensor ($L = 4$ mm; thickness = 1 mm) was glued onto four glass piles and mounted on a ceramic substrate (0.7 mm in thickness). This ensures a reasonable thermal isolation. It was placed in a circular tube with inner diameter of 32 mm, and turned by a computer controlled stepping engine. Optical feedback was used to define the 0° and 180° positions.

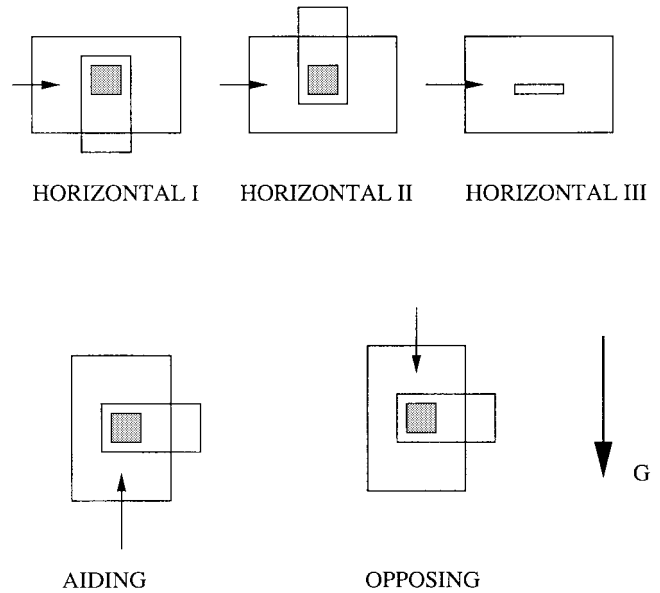


Fig. 3. The sensor in a circular tube with 32 mm internal diameter and the five orientations studied. The gravity force is depicted with the vector G . The smaller vectors indicate the direction of the forced flow component.

The electrical connections to the sensor were realized with a flexible connector. Every 8 s the sensor was turned around its axis. Data were sampled at 100 Hz and digitized by a 12 bit A–D converter before further analysis. Subsequent 8 s epochs were digitally subtracted to yield the ADM-flow signal. The turning of the sensor was realized within 0.5 s. The operating temperature of the sensor was about 90°C . All experiments were carried out using air with a temperature between 22°C and 24°C and at atmospheric pressure. The total measurement time per data-point was 5 min.

Flow was controlled using a flow controller (BROOKS; range 0–20 L/m). In practice, however, no flow velocities could be controlled below $Re = 17$ (mean velocity approximately 60 mm/s), and measurements were performed with $17 < Re < 140$.

D. Experimental Setup II

In order to measure flow in the mixed convective region with $Re \ll 17$, an experimental setup was realized that is illustrated in Fig. 4.

A computer controlled vertical piston was constructed, that can move back and forth in order to generate the airflow in two opposite directions. The number of rotations of the engine that moves the piston is measured by a hardware clock in the engine control unit (ECU). With this setup, we estimate the velocity error for velocities of 1 to 25 mm/s ($0.28 < Re < 7$) to be less than 1%.

The sensor was positioned in the center of a circular tube with inner diameter of 32×10^{-3} m that was placed perpendicular to the the piston, at a distance of about 0.1 m. This is well beyond the entrance length, that is estimated to be 0.01 m for the investigated flow velocities.¹

¹The entrance length can be estimated using $L_{entrance} \approx 0.035 \times D \times Re$, where D is the tube diameter.

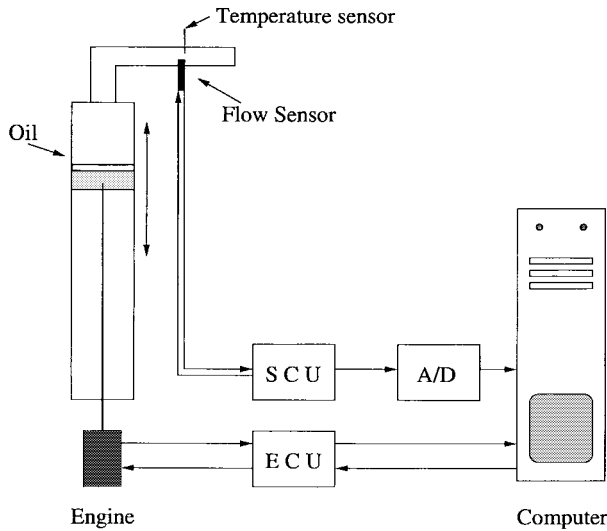


Fig. 4. Illustration of the measurement setup. ECU is the engine control unit, SCU the sensor control unit, and A/D the A–D converter. The sensor is placed in the tube that is perpendicular to the end of the piston. An oil layer is used to ensure zero air leakage at the piston.

The flow signal from the sensor control unit (SCU) is fed into the 12-bit A–D converter of the PC. A measurement protocol contained 100 measurements at different flow velocities, that were automatically set by the computer. For each flow velocity, the data were analyzed on-line, and only accepted if two criteria were satisfied. First, the (relative) standard deviation of the ADM-flow signal, σ_{ADM} , need to be smaller than 2.0% and secondly, the (relative) standard deviation of the measured number of rotations, σ_{engine} had to satisfy $\sigma_{engine} < 2.0\%$. The second criterion was added since in practice the number of rotations counted by the hardware clock on the ECU was sometimes disturbed by electromagnetic pulses that were present in our real-world environment. In this way, a completely automated measurement procedure was realized.

The mean flow velocity, v_0 , was calculated from the displacement of the cylinder per time unit, $\overline{v_{cylinder}}$, where the mean flow velocity in the measurement tube, $v_0 = \overline{v_{cylinder}} \times \frac{A_1}{A_2}$, with A_1 the area of the cylinder and A_2 the area of the measurement tube.

The gas temperature was measured using a temperature sensor that was placed directly opposite to the flow sensor and was found to be $25\text{ }^\circ\text{C} \pm 2\text{ }^\circ\text{C}$ throughout the measurement. Gas humidity was measured using a standard hygrometer and was $65 \pm 1\%$. Each session consisted of 100 data points in the flow region 1 to 25 mm/s. The measurements were repeated using two other sensors of the same silicon batch. The measurement time in each position A or B was about 14 s, yielding a new data point each 14 s.

III. RESULTS

Figs. 5 and 6 display the response curves and the ratio's of the output signal with respect to a ‘‘horizontal I’’ flow, respectively, for the five different orientations studied.

As shown in Fig. 5, for flows where $\log(Gr/Re^2) \geq -0.5$ an aiding flow yields the largest output signal, while an opposing flow yields smallest, even negative flow signals.

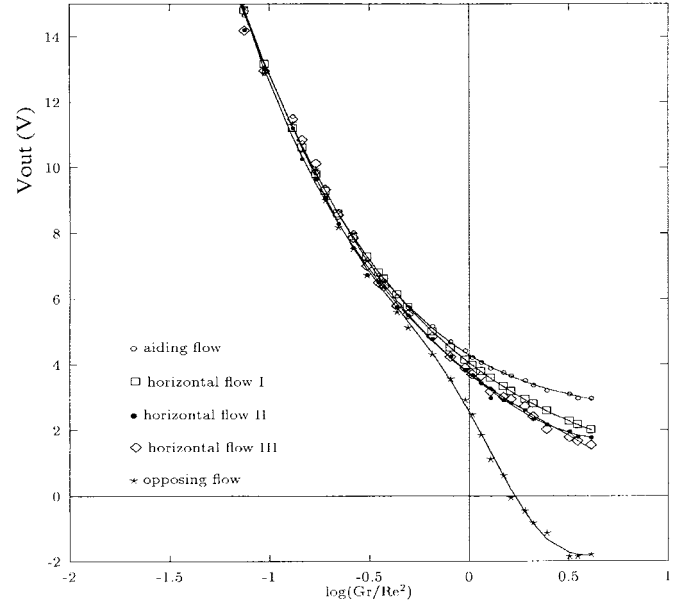


Fig. 5. Response curves for the five different orientations studied. Note that these values refer to *mean* values over the measurement interval of about 8 s.

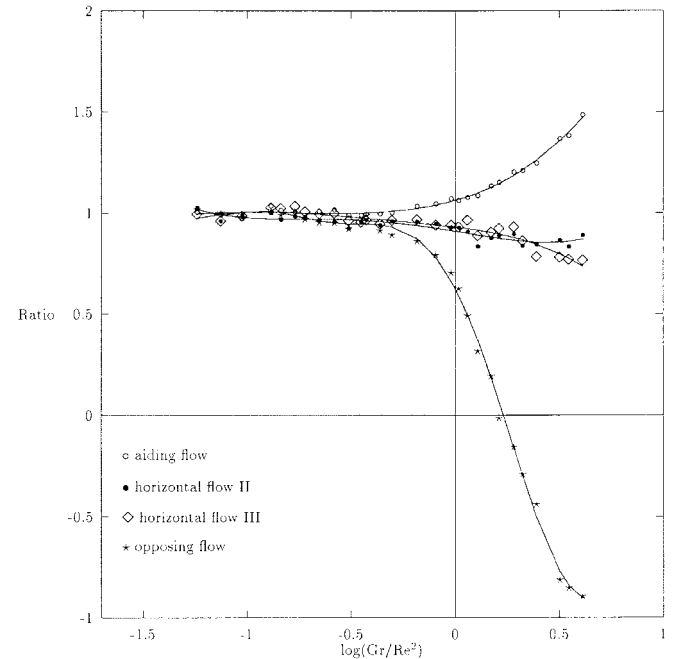


Fig. 6. Ratio of the displayed values for a vertical aiding (\circ), opposing (\star) and horizontal flows (type II \bullet and type III \diamond) as compared to horizontal flow type I.

The ratios of the different response curves, relative to a horizontal type I flow, are depicted in Fig. 6. At lower velocities (where $\log(Gr/Re^2) \gg -0.5$), the ratio for an aiding flow is larger than 1, indicating the aiding effect of the free convection, where for the other three flow types the ratio is less than one. For flows where $\log(Gr/Re^2) < -0.5$ the four curves merge.

We will consider a flow *effectively* purely forced if the ratio of its output signal as compared to a horizontal I flow is

TABLE I

LOWER LIMIT OF MIXED CONVECTIVE REGION FOR THE DIFFERENT FLOW ORIENTATIONS WITH RESPECT TO THE "HORIZONTAL I" FLOW DIRECTION. FOR THE OPERATING TEMPERATURE OF THE SENSOR, APPROXIMATELY 90 °C, WE FIND $Gr \approx 760$. Re_{crit} DENOTES THE CORRESPONDING REYNOLDS NUMBER BELOW WHICH THE MIXED CONVECTIVE REGION STARTS

Ratio	Gr/Re^2	Re_{crit}	v_{crit} (mm/s)
h2/h1	0.66 ± 0.05	34 ± 2	126 ± 8
h3/h1	0.50 ± 0.05	39 ± 2	144 ± 8
aid/h1	0.81 ± 0.05	31 ± 2	115 ± 8
opp/h1	0.26 ± 0.05	54 ± 6	200 ± 22

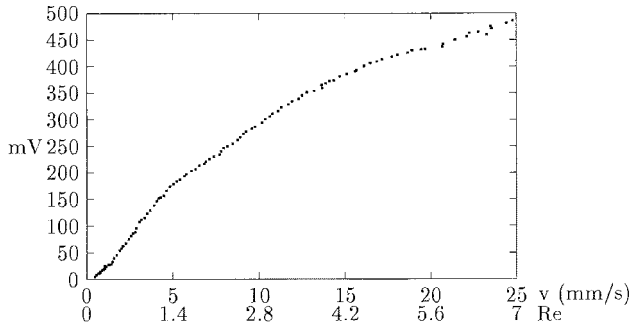


Fig. 7. Characteristics of the flow sensor mounted in a horizontal "flow I" position.

in the range [0.95–1.05]. Referring to Table I, we find that for $Gr/Re^2 > [0.3-0.8]$ there is an increasing significant contribution of the free convective forces to the flow field. A significant contribution of the buoyancy effects, therefore, occurs if $Re \ll 30$ or $v_0 \ll 100$ mm/s.

Fig. 7 presents the flow characteristic with the sensor in a horizontal "flow I" position. The mean flow velocity, v_0 , ranges from 1 to 25 mm/s ($0.3 \leq Re \leq 7$). As pointed out in the previous section, both the relative error in the velocity and the relative error in the measured data points are less than 2%. The total measurement time was approximately 6 h. No error bars are presented in the graph, since these have approximately the size of the dots. Throughout the measurement, the gas temperature was 25 ± 2 °C and the humidity $65 \pm 1\%$.

Fig. 8 illustrates the lower bound of flow detection. Two phenomena are shown. First, a flow velocity of 1 mm/s ($Re \approx 0.3$) is clearly detected. Secondly, due to experimental limitations, flow velocities below 0.5 mm/s could not reliably be generated.

Repeating the measurement with the same sensor showed differences less than 1–2% in the characteristics. We furthermore studied different sensors from the same batch in their individual responses. In this measurement the sensor was mounted in a 15 mm internal diameter tube. Below $v_0 = 100$ mm/s, the relative errors are less than 15%. For mean velocities $v_0 > 100$ mm/s, the errors are less than 3%. The larger differences at lower flow velocities are due to the small differences in sensor mounting that were present, resulting in slightly different orientations of the sensor with respect to the gravity vector. Since for flow velocities below 100 mm/s, there is a significant contribution of the free convection to the heat transfer, different orientations of the sensor will result in different characteristics below this flow velocity. This is illustrated in Fig. 9.

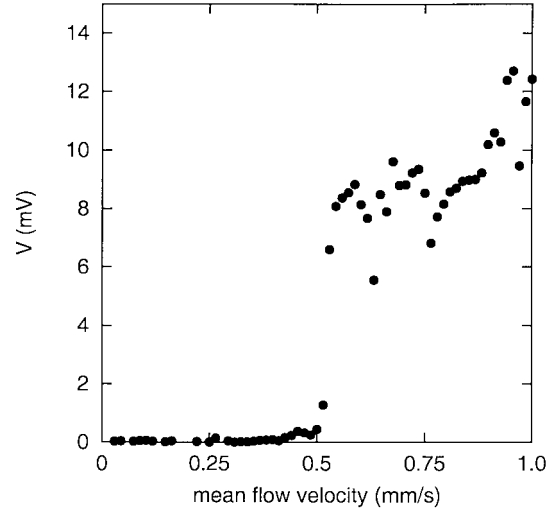


Fig. 8. Illustration of the onset of the detection of the flow. Flow detection starts around 0.5 mm/s ($Re \approx 0.15$) and is clearly detected at $v_0 = 1$ mm/s ($Re \approx 0.3$). Mechanical limitations caused the discontinuity at $v_0 = 0.55$ mm/s.

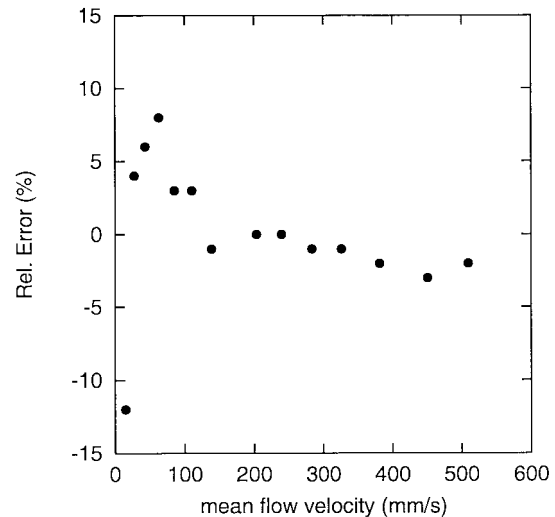


Fig. 9. Typical relative inter-sensor differences in the response curves as a function of the flow velocity.

IV. DISCUSSION AND CONCLUSIONS

Thermal flow measurements in the mixed convective region are complicated by a significant contribution of the natural convection to the velocity field [1]. Therefore, the output signal caused by natural convection may be of the same order or even larger than the signal generated by the forced flow component. Calibration procedures at zero flow conditions are not always possible in measurement situations where discontinuation of the flow is not feasible. Moreover, natural fluctuations in the heat transferred by free convection occur and drift in the electronic circuitry may be present. These phenomena make zero-flow calibration procedures, if possible at all, useless. Application of ADM almost completely eliminates the contribution of all these components making highly accurate ultralow flow measurements feasible.

Our experiments with the different orientations of the sensor w.r.t. the gravity vector define the upper bound of the mixed flow region. If we consider a flow *effectively* purely forced if the ratio of its output signal as compared to a “horizontal I” flow is in the range [0.95–1.05], we find that for $\text{Gr}/\text{Re}^2 > [0.3\text{--}0.8]$ there is a significant contribution of the free convective forces to the heat transfer and flow field. This is of the same order of magnitude as the value found by Sparrow [7] for his (2-D) analysis of a free plate, where the lower bound is found to be $\text{Gr}/\text{Re}^2 = 0.3$.²

We have presented the first characteristic of a silicon thermal air flow vector-sensor in the mixed convective region, with highly dominant buoyancy effects. By application of ADM very accurate ($\geq 98\%$) air flow measurements for Re numbers down to $\text{Re} = 0.3$ are feasible. This is a factor of 100 more sensitive than conventional hot wire flow measurements and about a factor 300–1000 more sensitive than any other measurement performed with thermal silicon flow sensors thus far. The time resolution is limited by the interval ΔT in between two successive measurements, which is in the order of seconds. (In our measurement ΔT was set to approximately 8 s). This makes the presented method especially suitable for high precision measurements in slowly varying flows.

Clearly, in practical applications measuring these low flow velocities, the sensor needs to be turned instead of the flow. For experimental reasons, however, we decided to build the computer controlled piston. With this equipment air speeds as low as 1 mm/s could be repeatedly and accurately induced. Moreover, these flow velocities are well below the lower limit of standard commercially available flow controllers, as was also pointed out in the methods section.

Applications are found in, e.g., high precision volume measurements, flow measurements in the building environment (for instance for draught measurements or ventilation studies), and flow measurements in low pressure environments.

ACKNOWLEDGMENT

The authors would like to thank Prof. H. E. A. van den Akker and VPIstruments (<http://www.vpinstruments.com>) for providing equipment and support.

REFERENCES

- [1] C. G. Lomas, *Fundamentals of Hot Wire Anemometry*. Cambridge, U.K.: Cambridge Univ. Press, 1986.
- [2] S. P. Lee and S. Ken Kauh, “A new approach to enhance the sensitivity of a hot-wire anemometer and static response analysis of a variable-temperature anemometer,” *Exper. Fluids*, vol. 22, pp. 212–219, 1997.
- [3] B. van Oudheusden, “Integrated silicon flow sensors,” Ph.D. dissertation, Delft University of Technology, Delft, The Netherlands, 1989.

²Their criterion for a flow to be effectively pure (either forced or free) is that the heat transfer coefficient deviates by no more than 5% from the value associated with the completely pure flow. We further remark that their results are obtained analytically for a free plate.

- [4] T. M. Betzner, J. R. Doty, A. M. A. Hamad, H. T. Henderson, and F. Berger, “Structural design and characteristics of a thermally isolated, sensitivity enhanced, bulk-micromachined silicon flow sensor,” *J. Micromech. Microeng.*, vol. 6, pp. 217–227, 1996.
- [5] C. Kwok, K. M. Lin, and R. S. Huang, “A silicon thermocapacitive flow sensor with frequency modulated output,” *Sens. Actuators A*, vol. 57, pp. 35–39, 1996.
- [6] K. Toda, I. Sanemasa, and K. Ishikawa, “Simple temperature compensation of thermal air-flow sensor,” *Sens. Actuators A*, vol. 57, pp. 197–201, 1996.
- [7] E. M. Sparrow, R. Eichhorn, and J. L. Gregg, “Combined forced and free convection in a boundary layer flow,” *Phys. Fluids*, vol. 2, no. 3, pp. 319–328, 1959.
- [8] A. F. P. van Putten, “Ambient temperature compensated double bridge anemometer,” U.S. Patent 4 548 077, 1985.
- [9] ———, “Device for measuring the flow velocity of a medium,” European Patent, 0 119 327, 1987.
- [10] ———, “Thermal feedback drives sensor bridge simultaneously with constant supply voltage and current,” *IEEE Trans. Instrum. Meas.*, vol. 39, pp. 48–51, 1990.
- [11] M. J. A. M. van Putten, M. H. P. M. van Putten, A. F. P. van Putten, J. C. Pompe, and H. A. Bruining, “A silicon bidirectional flow sensor for measuring respiratory flow,” *IEEE Trans. Biomed. Eng.*, pp. 205–208, 1997.
- [12] M. H. P. M. van Putten, M. J. A. M. van Putten, A. F. P. van Putten, and P. F. A. M. van Putten, “Method for drift elimination in sensors,” U.S. Patent 5 426 969 and European Patent application 94 202 293.0, 1995.
- [13] M. J. A. M. van Putten, M. H. P. M. van Putten, and A. F. P. van Putten, “Full additive drift elimination using the alternating direction method,” *Sens. Actuators A*, vol. 44, pp. 13–17, 1995.
- [14] ———, “Highly accurate flow measurements with thermal flow sensors using the alternating direction method,” in *Proc. IMTC*, 1996, vol. 1, pp. 527–530.

Michael J. A. M. van Putten was born in 1963. He received the M.Sc. degree in applied physics in 1989 from Delft University of Technology, Delft, The Netherlands and the M.D. degree (with honors) in 1991 from the University of Leiden,

Currently he is working at the Dept. of Neurology, Leiden University Hospital and at the Faculty of Applied Physics, Kramers Laboratorium voor Fysische Technologie, Delft University of Technology, studying silicon thermal flow sensors and their applications, for instance for respiratory flow measurements.

Maurice H. P. M. van Putten was born in 1964. He received the M.Sc. degree (with honors) in electrical engineering in 1986 from Delft University of Technology, Delft, The Netherlands, the M.Sc. degree in mathematical sciences in 1988 from the University of Delaware, Newark, and the Ph.D. degree from California Institute of Technology, Pasadena, in 1992 on the reformulation of Maxwell’s equations in constraint-free, covariant divergence form.

He is currently an Assistant Professor of Mathematics at the Massachusetts Institute of Technology, Cambridge.

Anton F. P. van Putten was born in 1939. He studied electrical engineering at Delft University of Technology, Delft, The Netherlands. He received the Ph.D. degree (with great distinction) in 1988 from the Katholieke Universiteit Leuven, Leuven, Belgium.

He has written a book on electronic measurement systems that is in its second edition. He holds several patents and has published various papers on silicon flow sensors. His main interests are doing research and teaching on sensors and actuators.